A low-cost time-hopping impulse radio system for high data rate transmission[1]

Andreas F. Molisch,[2] Ye Geoffrey Li, Yves-Paul Nakache, Philip Orlik,
Makoto Miyake, Yunnan Wu, Sinan Gezici, Harry Sheng,
S. Y. Kung, H. Kobayashi, H.Vincent Poor, Alexander Haimovich,and Jinyun Zhang[3]

[1] Part of this work was presented at WPMC 2003, Yokosuta, Japan.

[2] Author for correspondence. Email: Andreas.Molisch@ieee.org.

[3] A. F. Molisch, Y. P. Nakache, P. Orlik, and J. Zhang are with Mitsubishi Electric Research Labs, Cambridge, MA, USA. Y. G. Li is with Georgia Institute of Technology, Atlanta, GA, USA. M. Miyake is with Information Technology R&D Center, Mitsubishi Electric Corp., Ofuna, Japan..Y. Wu, S. Gezici, S. Y. Kung, H. Kobayashi, and H. V. Poor are with Princeton University, Princeton, NJ, USA. H. Sheng and A. Haimovich are with New Jersey Institute of Technology, Newark, NJ, USA.

Abstract

We present an efficient, low-cost implementation of time-hopping impulse radio that fulfills the spectral mask mandated by the FCC and is suitable for high-data-rate, short-range communications. Key features are: (i) all-baseband implementation that obviates the need for local oscillators and other passband components, (ii) symbol-rate (not chip rate) sampling, A/D conversion, and digital signal processing, (iii) fast acquisition due to novel search algorithms, (iv) spectral shaping that can be adapted to accommodate different spectrum regulations and interference environments. Computer simulations show that this system can provide 110Mbit/s at 7-10m distance, as well as higher data rates at shorter distances under FCC emissions limits. Due to the spreading concept of time-hopping impulse radio, the system can sustain multiple simultaneous users, and can suppress narrowband interference effectively.

I. Introduction

Ultrawideband (UWB) wireless systems are defined as systems that use either a large relative bandwidth (ratio of bandwidth to carrier frequency larger than 25%), or a large absolute bandwidth (larger than 500MHz). While UWB radar systems have been used for a long time, mainly in the military domain [1], UWB communications systems are a fairly recent development. The first papers in the open literature are those of Win and Scholtz [2], [3], [4], who developed the concept of time-hopping impulse radio (TH-IR) system. This concept excited immense interest in the area of military [5] as well as civilian [6] communications. Further advances of TH-IR are described, e.g., in [7], [8], [9], [10], [11]. In 2002, the FCC (Federal Communications Commission) in the US allowed *unlicensed* UWB communications [12]. This greatly increased commercial interest in UWB, leading to a large number of papers, see, e.g., [13], [14].

One of the most promising applications is data communications at rates that are higher than the currently popular 802.11b (11 MBit/s) and 802.11a ($<$54Mbit/s) standards. The goal, as mandated, e.g., by the standardization committee IEEE 802.15.3a, is a system that can provide multiple piconets with 110Mbit/s each. This data rate should be achieved for distances up to (Personal Area Networks). Higher data rates should be feasible at shorter distances.10m

The principle of using very large bandwidths has several generic advantages:

- By spreading the information over a large bandwidth, the spectral *density* of the transmit signal can be made very low. This decreases the probability of intercept (for military communications), as well as the interference to narrowband victim receivers.
- The spreading over a large bandwidth increases the immunity to narrowband interference and ensures good multiple-access capabilities [15], [16].
- The fine time resolution implies a high temporal diversity, which can be used to mitigate the detrimental effects of fading [17].
- Propagation conditions can be different for the different frequency components. For example, a wall might be more transparent in a certain frequency range. The large bandwidth increases the chances that at least some frequency components arrive at the receiver [18].

These advantages are inherent in the use of very large bandwidths, and can thus be achieved by *any* UWB system, including the recently proposed UWB frequency-hopping OFDM system [19] and UWB direct-sequence spread spectrum (DS-SS) systems [20]. However, TH-IR has additional advantages:

- Recent information-theoretic results indicate that higher capacities can be achieved than with DS-SS systems [21], [22].
- More important from a practical point of view, impulse radio systems operate in baseband only, thus requiring no mixers, local oscillators, etc. [7]. This allows an extremely low-cost implementation.

A lot of progress has been made in the theoretical understanding of impulse radio, as evidenced by the papers mentioned above. However, several assumptions made in the theoretical analyses do not agree with the requirements for a practical implementation of a high-data-rate impulse radio system. Those requirements may stem from the regulations by the FCC and other frequency regulators, from the necessity of coexistence with other devices, and from cost considerations. The goal of this paper is to describe the complete physical-layer design of an IR system that is suitable for practical implementation. In this system, we combine existing and innovative aspects, giving special attention to the interplay between the different aspects. The current paper is thus more of an “engineering” paper, while the theoretical background of some of our innovations is described in [23], [24], [25].

The remainder of the paper is organized the following way: in Section II, we present an overview of the system. Next, we discuss the transmit signal, and how its spectrum can be shaped to fit the requirements of regulators, as well as to minimize interference to nearby devices. Section IV describes the signal detection at the receiver, including the structure of the Rake receiver and the equalizer. The channel estimation procedure that is used for establishing the weights of the Rake receiver and equalizer is discussed in Section V. Finally, Section VI presents simulations of the total performance of the system in terms of coverage and resistance to interference from narrowband signals and other UWB transmitters. A summary and conclusions wrap up the paper.

II. System overview

The system that we are considering is a time-hopping impulse radio (TH-IR) system. We first describe "classical" TH-IR [4]. Each data bit is represented by several short pulses; the duration of the pulses determines essentially the bandwidth of the (spread) system. For the single-user case, it would be sufficient to transmit a single pulse per symbol. However, in order to achieve good multiple access (MA) properties, we have to transmit a whole sequence of pulses. Since the UWB transceivers are unsynchronized, so-called “catastrophic collisions” can occur, where pulses from several transmitters arrive at the receiver almost simultaneously. If only a single pulse would represent one symbol, this would lead to an extremely bad signal-to-interference ratio, and thus to high bit error probability BEP. These catastrophic collisions are avoided by sending a whole sequence of pulses instead of a single pulse. The transmitted pulse sequence is different for each user, according to a so-called time-hopping (TH) code. Thus, even if one pulse within a symbol collides with a signal component from another user, other pulses in the sequence will not. This achieves an interference suppression gain that is equal to the number of pulses in the system. Figure 1

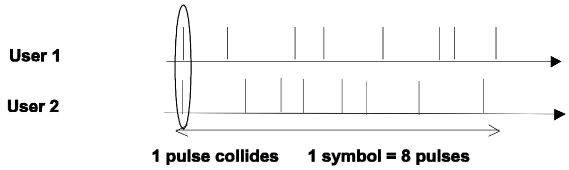

Fig. 1. Principle of time-hopping impulse radio for the suppression of catastrophic collisions.

shows the operating principle of a generic TH-IR system. We see that the possible positions of the pulses within a symbol follow certain rules: the symbol duration is subdivided into N_f "frames" of equal length. Within each frame the pulse can occupy an almost arbitrary position (determined by the time-hopping code). Typically, the frame is subdivided into "chips", whose length is equal to a pulse duration. The (digital) time-hopping code now determines which of the possible positions the pulse actually occupies. The modulation of this sequence of pulses can be pulse-position modulation (PPM), as suggested in [4], or amplitude modulation (PAM). PPM has the advantage that the detector can be simpler (an energy detector) in AWGN channels. However, reception in multipath environments requires a Rake receiver for either PPM or PAM.

While this scheme shows good performance for some applications, it does have problems for high-data rate, FCC-compliant systems:

1) Due to the use of PPM, the transmit spectrum shows spectral lines. This requires the reduction of the total emission power, in order to allow the fulfillment of the FCC mask within each 1MHz band, as required by the FCC.
2) Due to the high data rate required by 802.15, and due to the high delay spread seen by indoor channels, the system works better with an equalizer. An equalizer for PPM will introduce increased complexity and cost.
3) For a full recovery of all considered multipath components, the system requires a Rake receiver with a large number of fingers. A conventional implementation, using many digital correlators, will also introduce increased complexity and cost.
4) Due to the relatively low spreading factor of less than 40, the number of possible pulse positions within a frame is limited. This might lead to higher collision probability, and thus smaller interference suppression.

The first two problems are solved by using (antipodal) pulse amplitude modulation (PAM) instead of PPM. This eliminates the spectral lines, and allows in general an easier shaping of the spectrum. Furthermore, it allows the use of simple linear equalizers. As detailed below, an innovative Rake receiver is considered to overcome the third problem; this Rake structure implements correlators by means of pulse generators and multipliers only. The problem of multiple-access interference, finally, can be addressed by interference-suppressing combining of the Rake finger signals.

A block diagram of the system is shown in Figure 2. The transmit data stream is divided into blocks, and each block is encoded with a convolutional coder. We use a rate $1/2$ convolutional code with a constraint length 7.

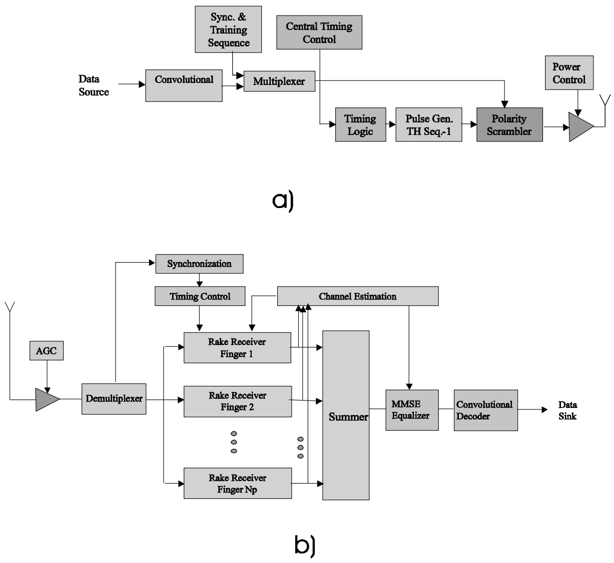

Fig. 2. Blockdiagram of the transmitter (a) and receiver (b).

The use of turbo codes or low-density parity check codes would improve the performance by approximately 2 dB; however, decoding becomes challenging at the high data rates envisioned in this scheme. Then, a preamble is prepended that can be used for both acquisition and channel estimation. As mentioned above, the modulation and multiple access format is BPSK-modulated TH-IR. Each pulse sequence representing one symbol is multiplied by ± 1, depending on the bit to be transmitted. Finally, each data block (including preamble) is amplified (with power control, in order to minimize interference to other systems), and transmitted. Note that as the system is packet based and the number of packets per second can vary, it is not desirable to code across packets.

In the receiver, the acquisition part of the preamble is stripped off and used to determine the timing. Once this has been established, the "channel estimation part" of the preamble is used to determine the coefficients for the Rake receiver and the equalizer. Matched-filter detection is firstly applied to the received signal in the main data part, where the filter is matched to both the pulse shape and the time-hopping sequence. The signals in the main body of the data block are first match-filtered by the time-hopped sequence. This matches the received signal both to the pulseshape and the time-hopping sequence. The matched-filtered signal is then sent through a Rake receiver. We use here an innovative structure that requires only pulse generators and no delays to do both the matched filtering and the Rake reception, which makes an analogue implementation possible. – this allows us to perform the sampling and A/D conversion only at the *symbol rate*, instead of the chip rate. Note that for chip rate sampling, A/D converters with about 20Gsamples/s would be required. The outputs of the Rake fingers are weighted (according to the principles of optimum combining) and summed up. The optimum location and weight of the fingers can be determined from the channel sounding sequence, which is processed before the reception of the actual data. The output of the summer is then sent through an MMSE equalizer and a decoder for the convolutional code.

One important point of the system is that all the pulses are *baseband* pulses, more specifically, derivatives of Gaussian pulses. This allows a simple pulse generation, and obviates any need for passband components and local oscillators. This is a typical property of time-hopping impulse radio; however, it is not a trivial task within the restrictions of the FCC that the main power is emitted in the 3-10GHz range. We will show in Sec. 3 how this can be achieved.

The goal of our design is to obtain a low-cost implementation. Thus, the design is not theoretically optimum, but rather contains a number of simplifications that reduce complexity of implementation and costs.

III. Transmit signal and spectral shaping

A. Mathematical description of the transmit signal

Throughout this paper, we use a communication system model where the transmitted signal is given by

$$s_{tr}(t) = \sum_{j=-\infty}^{\infty} d_j b_{\lfloor j/N_f \rfloor} w_{tr}(t - jT_f - c_j T_c) = \sum_{k=-\infty}^{-\infty} b_k w_{seq}(t - kT_s) \tag{1}$$

where w_{tr} is the transmitted unit-energy pulse, T_f is the average pulse repetition time, N_f is the number of pulses representing one information symbol of length T_s, and b is the information symbol transmitted, i.e., ± 1. w_{seq} is the pulse sequence transmitted representing one symbol. The TH sequence provides an additional time shift of $c_j T_c$ seconds to the j^{th} pulse of the signal, where T_c is the chip interval. To prevent pulses from overlapping, the chip interval is selected to satisfy $T_c \quad \leq \quad T_f / N_c$. We also allow "polarity scrambling" (see Sec. III.4), where each pulse is multiplied by d_j.

An alternative representation can be obtained by defining a sequence $\{s_j\}$ as follows

$$s_j = \begin{cases} d_{\lfloor j/N_c \rfloor} & \text{for} \quad j - N_f \lfloor j/N_c \rfloor = \mathrm{c}_{\lfloor j/N_c \rfloor} \\ 0 & \text{otherwise} \end{cases} \tag{2}$$

Then, assuming $T_f \,/\, T_c = N_c$, without loss of generality, the transmit signal can be expressed

$$s_{tr}(t) = \sum_{j=-\infty}^{\infty} s_j b_{\lfloor j/N_f N_c \rfloor} w_{tr}(t - jT_c). \tag{3}$$

To satisfy the spectrum masking requirement of the FCC, the transmit waveform w_{tr}, also known as monocycle waveform, is chosen to be the 5th derivative of the Gaussian pulse and it can be expressed as,

$$w_{tr}(t) = p(t) = K_2 \left(-15 \frac{t}{\sigma_p} + 10 \frac{t^3}{\sigma_p^3} - \frac{t^5}{\sigma_p^5} \right) \exp\left(-\frac{t^2}{2\sigma_p^2}\right), \tag{4}$$

where K_2 is a normalization constant, and σ_p controls the width of the pulse and it is chosen according to the spectral mask requirement of the FCC, which is [26],

$$\sigma_p = 5.08 \times 10^{-11}. \tag{5}$$

Other signals shapes are possible; in particular, a combination of weighted pulses $p(t)$ (as explained below) can be used to improve the spectral properties. The various methods (e.g., Rake receiver, pulse polarity randomization, ...) discussed in the remainder of the paper can be applied independently of the exact shape of the transmit waveform.

B. Spectral shaping - general aspects

One of the key requirements for a UWB system is the fulfillment of the emission mask mandated by the national spectrum regulators. In the USA, this mask has been prescribed by the FCC and essentially allows emissions in the 3.1-10.6 GHz range with power spectral density of -41.3 dBm/MHz; in Europe and Japan, it is still under discussion. In addition, emissions in certain parts of the band (especially the $5.2 - 5.8$ GHz range used by wireless LANs) should be kept low, as UWB transceivers and IEEE 802.11a transceivers, which operate in the 5GHz range, are expected to work in close proximity. We are using two techniques in order to fulfill those requirements.

- The first is a linear combination of a set of basis pulses to be used for shaping of the spectrum of a transmitted impulse radio signal. The delayed pulses are obtained from several appropriately timed programmable pulse generators. The computation of the delays and weights of those pulses is obtained in a two-step optimization procedure [23].
- A further improvement of the spectral properties can be obtained by exploiting different polarities of the pulses that constitute a transmit sequence w_{seq}. Using different pulse polarities does not change anything for the signal detection, as it is known at the receiver, and can thus be easily reversed. However, it does change the spectrum of the *emitted* signal, and thus allows a better matching to the desired frequency mask [24].

The first technique (combination of pulses) leads to a shaping of the spectrum, allowing the placement of broad minima and an efficient “filling out” of the FCC mask. The second technique is used to reduce or eliminate the peak-to-average ratio of the spectrum, and allow the design of more efficient multiple-access codes. Note that these two aspects are interrelated, and the optimization of pulse combination and polarity randomization should be done jointly in order to achieve optimality. However, such a joint treatment is usually too complicated for adaptive modifications of the transmit spectrum.

A further important aspect of the spectral shaping is that it can be used not only to reduce interference to other devices, but also interference $from$ narrowband interferers. This can be immediately seen from the fact that matched filtering is used in the receiver. Placing a null in the transmit spectrum thus also means that the receiver suppresses this frequency. Furthermore, it might be advantageous in some cases to perform "mismatched filtering" at the receiver by placing minima in the receive transfer function even if there is no corresponding minimum in the transmit spectrum. This is useful especially for the suppression of narrowband interferers that could otherwise drive the A/D converter into saturation.

C. Pulse combination

One of the key problems of “conventional” TH-IR radio is that it is difficult to influence its spectrum without the use of RF components. Spectral notches, e.g., are typically realized by means of bandblock filters. However, this is undesirable for extremely low cost applications; furthermore, it does not allow adaptation to specific interference situations. We have thus devised a new scheme for shaping the spectrum [23]. This scheme uses delaying and weighting of a set of basis pulses to influence the transmit spectrum.

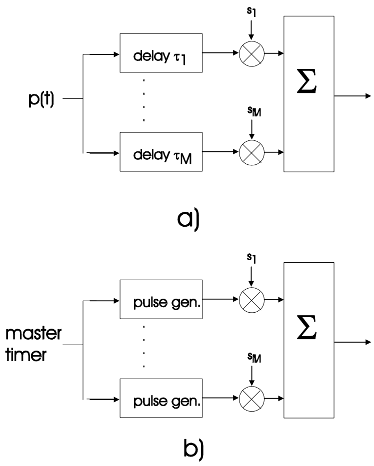

Fig. 3. Principle of pulse combination for spectral shaping with delay lines (a) and with programmable pulse generators (b).

The basic transmit waveform w_{tr} is a sum of delayed and weighted "basic pulse shapes" $p(t)$ that can be easily generated, e.g., Gaussian pulses and their derivatives.

$$w_{tr}(t) \equiv \sum_{i=0}^{M} u_i p(t - \xi_i) \tag{6}$$

$$W(j\Omega) \equiv \int_{-\infty}^{\infty} w_{tr}(t) e^{-j\Omega t} dt = \sum_{i=0}^{M} u_i P(j\Omega) e^{-j\Omega \xi_i}. \tag{7}$$

where W is the Fourier transform of w_{tr}, and Ω is the transform variable. In contrast to tapped delay lines, where only certain discrete delays are feasible, we assume here that a continuum of delays can be chosen. This can be achieved by the use of programmable pulse generators. The range of allowed delays of the coefficients is determined by the pulse repetition frequency of the communication system. The number of pulse generators $M + 1$ should be kept as low as possible to reduce the interference.

Let us introduce the following notations:

$$\underline{u} \equiv [u_0 \; u_1 \; \ldots \; u_M]^T \tag{8}$$

$$\underline{\xi} \equiv [\xi_0 \; \xi_1 \; \ldots \; \xi_M]^T \tag{9}$$

$$r(\lambda) \equiv \int_{-\infty}^{\infty} p(t - \lambda) p(t) dt = r^*(-\lambda), \tag{10}$$

$$\mathbf{R}(\underline{\xi}) \equiv \begin{pmatrix} r(0) & r(\xi_0 - \xi_1) & \cdots & r(\xi_0 - \xi_M) \\ r(\xi_1 - \xi_0) & r(0) & \ddots & r(\xi_1 - \xi_M) \\ \vdots & \ddots & \ddots & \vdots \\ r(\xi_M - \xi_0) & r(\xi_M - \xi_1) & \cdots & r(0) \end{pmatrix}, \tag{11}$$

$$\langle w_{tr}(t), w_{tr}(t) \rangle \equiv \int_{-\infty}^{\infty} w_{tr}(t) w_{tr}^*(t) dt = \underline{u}^H \mathbf{R}(\underline{\xi}) \underline{u} \tag{12}$$

where the superscript ^{H} denote Hermitian transposition.

The single user spectrum shaping problem can now be formulated as follows:

$$\max_{\underline{u},\underline{\xi}} \langle w_{tr}(t), w_{tr}(t)\rangle, \text{ subject to } |W(j\Omega)|^2 \leq M(\Omega) \ , \forall\Omega \in [-\infty, \infty]. \tag{13}$$

where $M(\Omega)$ is the upper-bound on the magnitude response regulated by FCC. This is equivalent to:

$$\min_{\underline{u},\underline{\xi}} \max_{\Omega\in[-\infty,\infty]} \frac{|W(j\Omega)|^2}{M(\Omega)}, \qquad \text{subject to } \underline{u}^H R(\underline{\xi})\underline{u} = 1. \tag{14}$$

The criteria for the optimization $M(\Omega)$ can thus stem from the FCC spectral mask, which is fixed, from the necessity to avoid interference to other users, which can be pre-defined or time-varying, or following an instantaneous or averaged determination of the emissions of users in the current environment, or other criteria. In any case, these criteria are mapped onto an "instantaneous' spectral mask that has to be satisfied by the pulse. If the fulfillment of the FCC spectral mask is the only requirement, then the optimum weights can be computed a priori, and stored in the transceivers; in that case, the computation time determining the optimum weights and delays is not relevant, and exhaustive search can be used. However, in order to adjust to different interference environments, a capability to optimize the weights dynamically is desirable. This can be achieved, e.g., by an efficient two-step procedure that in the first step uses an *approximate* formulation of the optimization problem, namely 2-norm minimization that can be solved in closed form. This solution is then used as the initialization of a nonlinear optimization (e.g., by means of a neural network) to find the solution to the *exact* formulation. Details of this two -step procedure can be found in [23]. Note also that the spectral shaping can be refined even more by combining different basis pulses. However, this requires different pulse generators, which increases implementation complexity.

D. *Polarity randomization*

Conventional impulse radio systems use only a pseudo-random variation of the pulse position to distinguish between different users. For PAM - TH-IR, the spectrum of the transmit signal is determined by the spectrum of the transmit waveform $w_{tr}(t)$, multiplied with the spectrum of the TH sequence. Figure 4 shows an example of a spectrum with a short (4 frames) time hopping sequence, in combination with a 5th-order Gaussian basis pulse. We can observe strong ripples, so that the peak-to-average ratio is about 6dB. However, the ideal case would be to find TH sequences whose spectrum is flat, so that the we can design the transmit waveform to fit the spectral mask as closely as possible. One way to achieve this goal is to use very long TH sequences (much longer than a symbol duration). However, this complicates the design of the receiver, especially the equalizer. Alternatively, we can use more degrees of freedom in the design of short sequences by allowing different amplitudes and polarities of the pulses for the design of the sequence. This helps to limit the power back-off by reducing the peak to average ratio. However, it is still true that the less pulses compose the sequence, the larger is the peak-to-average ratio. An example can be seen in Figs. 4 (unipolar sequence) and Fig. 5 (polarity randomization); it is obvious that the ripples have been considerably reduced; specifically, we reduced the crest factor by 1.6 dB. We also have to bear in mind that we need to generate a multitude of sequences that all should have the desired spectral properties, as well as approximate orthogonality with respect to each other for arbitrary time shifts of the sequences. This is a complex optimization problem, and has to be solved by an exhaustive search.

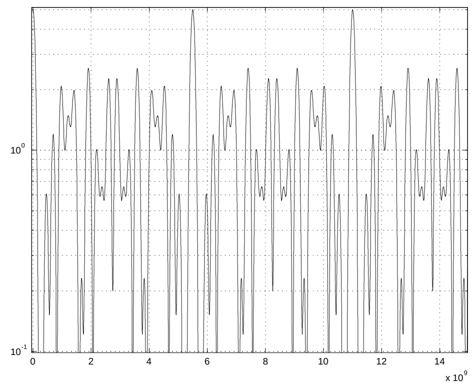

Fig. 4. Spectrum of time hopping sequence with "classical" TH sequence. 5 chips each in 5 frames. Positions of the pulses given by posit=[1 0 0 0 0 0 0 0 1 0 0 0 1 0 0 0 0 1 0 0 0 0 0 1 0].

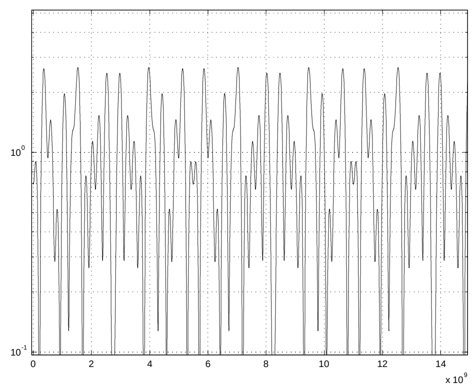

Fig. 5. Spectrum of PAM signal with polarity randomization of the TH sequence. Same positions of the pulses as in Fig. 4, but amplitudes of the pulses given by amp = [-0.5 0.5 0.5 -0.5 1.5].

IV. Signal detection

A. Received Signal and Rake reception

The Rake receiver is a key aspect of ultrawideband systems.[1] Due to the ultra wide bandwidth, UWB systems have a very fine temporal resolution, and are thus capable of resolving multipath components that are spaced at an inverse of the bandwidth. This is usually seen as a big advantage of UWB. Multipath resolution of components reduces signal fading because the multipath components are different diversity paths. The probability that the components are simultaneously all in a deep fade is very low. However, the fine time resolution also means that many of the multi-path components (MPC) have to be “collected” by the Rake receiver in order to obtain all of the available energy. A channel with N_p resolvable paths requires N_p fingers to collect all of the available energy. In a dense multi-path environment, the number of MPC increases linearly with the bandwidth. Even a sparse environment, such as specified by the IEEE 802.15.3a standard channel model [27], requires up to 80 fingers to collect 80% of the available energy.

[1] An exception are OFDM-based UWB systems, which use a different principle to collect the multipath energy [19].

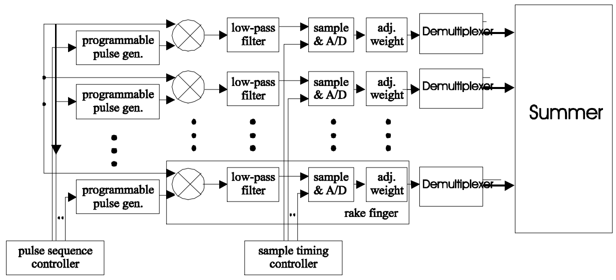

Fig. 6. Structure of Rake receiver for impulse radio.

Another problem is the complexity of the Rake fingers. In the conventional Rake finger of a direct-sequence-spread spectrum (DS-SS) system, the received signals is filtered with a filter matched to the chip waveform, and then in each Rake finger, correlated to time-shifted versions of the spreading sequence. In order to do the correlation, the signal first has to be sampled and analog-to-digital (A/D) converted at the chip rate. Then, those samples have to be processed. This involves convolution with the stored reference waveform, addition, and readout. Sampling and A/D converting at the chip rate, e.g., 10 Gsamples/s, requires expensive components.[2]

We avoid those problems by utilizing a Rake structure as outlined in Fig. 6. Each finger includes a programmable pulse generator, controlled by a pulse sequence controller. The signal from the pulse generator is multiplied with the received signal. The output of the multiplier is then sent through a low-pass filter, which generates an output proportional to a time integral of an input to the filter. The implementation is analogue, while the adjustable delay blocks have been eliminated. The hardware requirements for each Rake finger are: one pulse generator (which can be controlled by the same timing controller), one multiplier, and one sampler / AD converter. In the following, we assume the use of 10 Rake fingers; this is a very conservative number. Obviously, a larger number of Rake fingers would give better performance; this is one of the complexity/performance trade-offs in our design.

Next, we compute the output of the different Rake fingers. Let the impulse response of a UWB channel be

$$h\left(t\right) = \sum_{k} \alpha_k \delta\left(t - \tau_k\right), \tag{15}$$

where τ_k and α_k are the delay and (real) gain of the k-th path of the UWB channel, respectively. Then the channel output can be expressed as

$$x\left(t\right) = h\left(t\right) * s_{tr}\left(t\right) + n\left(t\right) = \sum_{n=-\infty}^{\infty} b_n \widehat{h}\left(t - nT_s\right) + n(t), \tag{16}$$

where

$$\widehat{h}\left(t\right) = \sum_{k} \alpha_k w\left(t - \tau_k\right). \tag{17}$$

[2]Note that some companies have proposed the use of *one-bit* A/D converters with $7.5 - 20$ Gsamples per second [20].

The output of the matched filter can be expressed as

$$y\left(t\right)=x\left(t\right)*w_{tr}\left(-t\right)=\sum_{k=-\infty}^{\infty}b_{k}\tilde{h}\left(t-kT_{s}\right)+\tilde{n}\left(t\right), \tag{18}$$

where

$$\tilde{h}\left(t\right)=\int\widehat{h}\left(t-\tau\right)w_{tr}\left(-\tau\right)d\tau=\sum_{k}\alpha_{k}r\left(t-\tau_{k}\right), \tag{19}$$

$$r\left(t\right)=\int w\left(t+\tau\right)w\left(\tau\right)d\tau, \tag{20}$$

and

$$\tilde{n}\left(t\right)=n\left(t\right)*w\left(-t\right). \tag{21}$$

The samples of the matched filter output can be thus written as

$$y[n]=y\left(n\Delta\right)=\sum_{k=-\infty}^{\infty}b_{k}\tilde{h}\left(n\Delta-kp\Delta\right)+\tilde{n}\left(n\Delta\right), \tag{22}$$

where Δ is the minimum time difference between Rake fingers and $p=T_s/\Delta$.

B. *Combining of the Rake finger signals*

Let $\tilde{h}\left(n_l\Delta\right)$'s, for $l=1,\ldots,L$ be the L taps with the largest absolute values, $\left|\tilde{h}\left(n_l\Delta\right)\right|$'s. The output of the Rake receiver can be expressed as

$$z\left[n,n_o\right]=\sum_{l=1}^{L}\gamma_l y\left[pn+n_l+n_o\right], \tag{23}$$

where γ_l is the weight for the l-th finger and n_o is a time offset. It is obvious that the signal quality of the Rake receiver output depends on the weight and initial time offset.

Maximal ratio combining (MRC) is a traditional approach to determine the weights of the Rake combiner. For the MRC Rake combiner, $\gamma_l=\tilde{h}\left(n_l\Delta\right)$, and

$$z\left[n,n_o\right]=\sum_{l=1}^{10}\tilde{h}\left(n_l\Delta\right)y\left[pn+n_l+n_o\right]. \tag{24}$$

Minimum mean-square-error (MMSE) Rake combining can improve the performance of the Rake receiver in the presence of interference. For the MMSE Rake combiner, the weights are determined to minimize

$$E\left|z[n,n_o]-b_n\right|^2. \tag{25}$$

The performance of the Rake receiver can be further improved if *adaptive timing* is used with the MMSE Rake combiner. That is, the goal is to find optimum time offset n_o and γ_l to minimize

$$E\left|z[n,n_o]-b_n\right|^2. \tag{26}$$

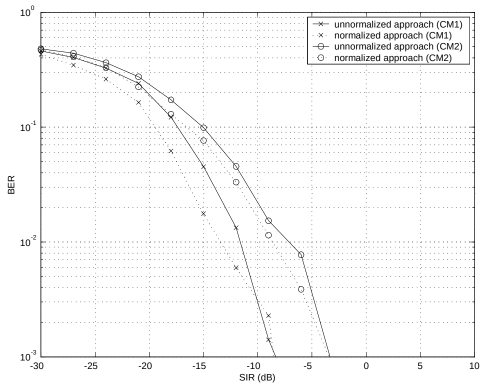

Fig. 7. Interference suppression performance.

When there is co-channel interference, the received signal can be written as

$$\bar{y}[n] = \sum_{k=-\infty}^{\infty} b_k \tilde{h}\left(n\Delta - kT_s\right) + \underbrace{\sum_{k=-\infty}^{\infty} \bar{b}_k \bar{h}\left(n\Delta - kT_s\right) + \tilde{n}\left(n\Delta\right)}_{i[n]} = \sum_{k=-\infty}^{\infty} b_k \tilde{h}\left(n\Delta - kp\Delta\right) + i\left[n\right], \quad (27)$$

where $\{\bar{b}_k\}$ and $\bar{h}\left(n\Delta - kT_s\right)$ are, respectively, i.i.d. sequence and channel impulse response corresponding to the interferer. It can be shown that $i\left[n\right]$ is not stationary but rather cyclo-stationary. Let

$$P_k = E\left\{\left|i\left[mp+k\right]\right|^2\right\}, \quad (28)$$

for any integer m and $k = 0, 1, \ldots, p-1$. Therefore, we need to normalize the channel impulse response corresponding to the desired signal by

$$\hat{h}\left(n\Delta\right) = \frac{\tilde{h}\left(n\Delta\right)}{\sqrt{P_k}}, \quad (29)$$

and then find the L taps with the largest absolute values of channel taps, $\left|\hat{h}\left(n_l\Delta\right)\right|$'s for the Rake receiver.

Figure 7 demonstrates the interference suppression performance for a UWB system with one interferer and 50 dB SNR. We compare the BER without normalization to the improved one that is normalized by noise power as described above.

C. Channel Equalizer

The combination of the channel and the Rake receiver constitutes an equivalent channel; however, since the symbol duration is shorter than the delay spread of the channel, intersymbol interference (ISI) does occur. We combat that by means of a MMSE (minimum mean square error) equalizer. The reasons for choosing a linear equalizer, instead of a DFE, are twofold:

- the system is intended to operate at symbol error probabilities of 1-10%; strong coding is used to decrease the frame error probability. Thus, a decision feedback of the "raw symbols" (hard decision before the decoder) would result in strong error propagation.

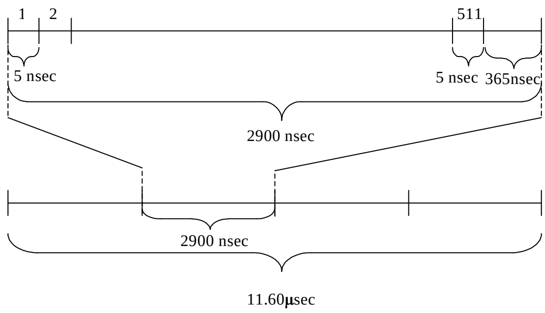

Fig. 8. Structure of the training sequence.

- the alternative to use the symbols after decision would require re-encoding and re-modulation before subtraction. This increases complexity considerably. As the ISI is not a dominant source of errors in our system, the possible gains from this improved DFE scheme do not warrant such an increase in complexity.

After the Rake receiver, a linear equalizer is used to mitigate residual interference. Let the coefficients of the equalizer be $\{c_{-K}, c_{-K+1}, \ldots.c_{-1}, c_0, c_1, \ldots..c_K\}$. Then the equalizer output is

$$\tilde{b}[n] = \sum_{k=-K}^{K} c_k z\left[n-k, n_o\right]. \tag{30}$$

To optimize performance, the equalizer coefficients are chosen to minimize the MSE of its output, that is

$$MSE = E\left|\tilde{b}[n] - b_n\right|^2. \tag{31}$$

V. Parameter estimation

A training sequence is used to determine the parameters for the Rake receivers and equalizers. It is desirable to use the correlators and A/D converters of the Rake receivers, since these components have to be available anyway. This is not straightforward, as the sampling and A/D conversion of the correlator outputs is done at the symbol rate, while the channel parameters have to be available for each possible chip sampling instant. This problem is solved by combining a "sliding correlator" approach with a training sequence that exhibits a special structure, as shown in Fig. 8.

A. Channel Estimation

The matched filter in the Rake receiver in UWB systems is implemented using analog circuits since it needs to operate at a high speed. The output of the matched filter is sampled at symbol rate ($1/T_S = 1/(p\Delta)$). Therefore, during each symbol period, we can only observe L outputs, each from one of L fingers. On the other hand, we need to estimate channel coefficients every Δ seconds; thus we need to obtain p uniform samples during each symbol period.

In order to solve this seeming paradox, we use an approach that shows some similarity to the “swept time delay cross correlator” channel sounder proposed in [28]. We send the same training sequence (with guard interval) multiple times to obtain denser sampling of the matched filter output. Specifically, in our case, we use four repetitions of the training sequence (see also Fig. 8), since $p = 32$, and $L = 10$ for our choice of parameters. Each training sequence consists of 511 symbols, and 365 ns guard interval to prevent interference caused by delay spread of UWB channels between adjacent training sequences. Consequently, the length of the whole training period for parameter estimation is $4(511 * 5 + 365) = 11600ns$ or $11.6\ \mu s$.

To obtain uniform samples, the timing of the l-th finger corresponding to the m-th training sequence is adjusted as follows:

$$t_{l,m} = 4(l-1)\Delta + (m-1)\Delta, \tag{32}$$

for $l = 1, \cdots, 10$, and $m = 1, \cdots, 4$.

Let the training sequence be b_k^t's for k=0, 1, ..., 510, where superscript ^{t} denotes "training". Then the training signal can be expressed as

$$s^t(t) = \sum_{k=0}^{510} b_k^t w(t - kT_s), \tag{33}$$

From Equation (22), the Δ-spaced output of the matched filter is

$$y^t(n\Delta) = \sum_{k=0}^{510} b_k^t \tilde{h}(n\Delta - kp\Delta) + \tilde{n}(n\Delta). \tag{34}$$

Consequently, channel parameters can be directly estimated by

$$\tilde{h}(n\Delta) = \frac{1}{511} \sum_{k=0}^{510} b_k^t y^t(n\Delta + kp\Delta). \tag{35}$$

To exploit the improved approach for UWB systems with co-channel interference, interference power has to be estimated. Using the estimated channel and the training sequence, the interference can be estimated by

$$i_t[n] = y_t(n\Delta) - \sum_{k=0}^{510} b_k^t \tilde{h}(n\Delta - kp\Delta), \tag{36}$$

and from it, interference power can be estimated by

$$P_k = \frac{1}{511} \sum_{m=0}^{510} |i_t[mp+k]|^2, \tag{37}$$

for $k = 0, 1, \ldots, (p-1)$.

Figure 9 shows the performance of our channel estimation. From Fig. 9(a), the channel estimation improves with the signal-to-noise ratio when it is less than 25 dB. However, when it is over 35 dB, there is an error floor. Fig. 9(b) shows the normalized MSE (NMSE) of the 10 largest channel taps, which is much better than the NMSE of overall channel estimation.

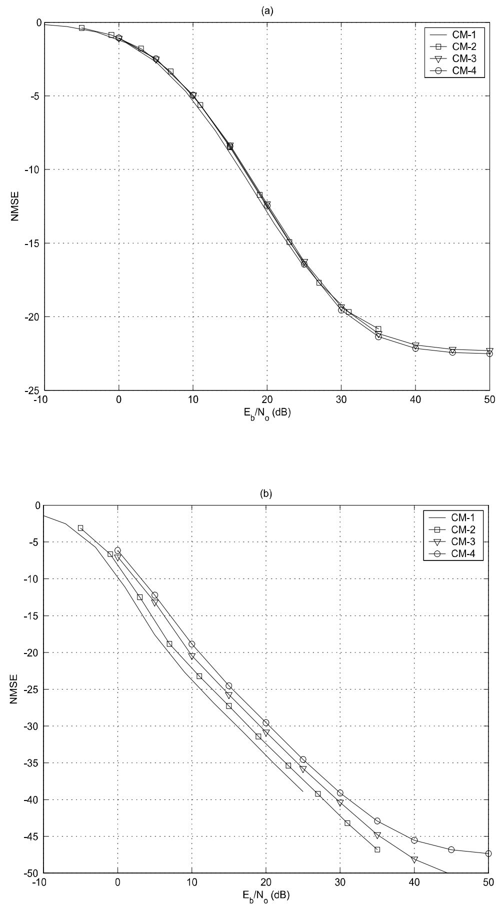

Fig. 9. NMSE of (a) overall channel estimation and (b) 10 largest channel taps

B. Rake Weight Estimation

Let $n_1, \cdots, n_L$ be the indices of the L largest taps. Then the weights for the MMSE Rake combiner and optimum timing can be found by minimizing

$$MSE(\vec{\gamma}, n_0) = \frac{1}{511} \sum_{n=0}^{510} \left| z_t(n, n_0) - b_n^t \right|^2 = \frac{1}{511} \sum_{n=0}^{510} \left| \sum_{l=1}^{10} \gamma_l y_t(pn + n_l + n_0) - b_n^t \right|^2 \tag{38}$$

Direct least-squares calculation yields that

$$\vec{\gamma} = \begin{pmatrix} \gamma_1 \\ \vdots \\ \gamma_{10} \end{pmatrix} = \left(\mathbf{Y}_t \mathbf{Y}_t^H \right)^{-1} \left(\mathbf{Y}_t \mathbf{b}_t^H \right), \tag{39}$$

where

$$\mathbf{Y}_t = \begin{pmatrix} y_t\left[n_1+n_o\right] & \cdots & y_t\left[510p+n_1+n_o\right] \\ y_t\left[n_2+n_o\right] & \cdots & y_t\left[510p+n_2+n_o\right] \\ \vdots & \cdots & \vdots \\ y_t\left[n_{10}+n_o\right] & \cdots & y_t\left[510p+n_{10}+n_o\right] \end{pmatrix}, \tag{40}$$

and

$$\mathbf{b}_t = \begin{pmatrix} b_0^t & b_1^t & \cdots & b_{510}^t \end{pmatrix}. \tag{41}$$

C. Equalizer Coefficient Estimation

From the estimated weights for the Rake receiver, its output can be calculated by

$$z_t\left[n, n_o\right] = \sum_{l=1}^{10} \gamma_l y_t\left[pn + n_l + n_o\right]. \tag{42}$$

The equalizer coefficients can be estimated by minimizing

$$\frac{1}{511}\sum_{n=0}^{511}\left|\sum_{k=-L}^{L} c_k z_t[n-k, n_o] - b_k^t\right|^2. \tag{43}$$

Consequently,

$$\begin{pmatrix} c_{-2} \\ \vdots \\ c_2 \end{pmatrix} = \left(\frac{1}{511}\sum_{k=0}^{510} \mathbf{z}_k^t \mathbf{z}_k^{t\,T}\right)^{-1} \left(\frac{1}{511}\sum_{k=0}^{510} \mathbf{z}_k^t b_k^t\right), \tag{44}$$

where

$$\mathbf{z}_k^t = \begin{pmatrix} z_t\left[k+2, n_o\right] \\ \vdots \\ z_t\left[k-2, n_o\right] \end{pmatrix}. \tag{45}$$

D. Synchronization

Before any data demodulation can be done on the received UWB signal, the template signal and the received signal must be time-aligned. The aim of acquisition is to determine the relative delay of the received signal with respect to the template signal. The conventional technique to achieve this is the serial search algorithm. In this scheme, the received signal is correlated with a template signal and the output is compared to a threshold. If the output is lower than the threshold, the template signal is shifted by some amount, which usually is comparable to the resolvable path interval and the correlation with the received signal is obtained again. In this way, the search continues until an output exceeds the threshold. If the output of the correlation comes from a case where signal paths and the template signal are aligned, it is called a signal cell output. Otherwise, it is called a non-signal cell

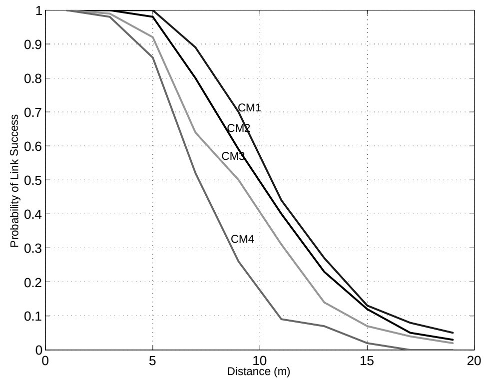

Fig. 10. Probability of link success as function of distance for 110Mbit/s mode

output. A false alarm occurs when a non-signal cell output exceeds the threshold. In this case, time t_p elapses until the search recovers again. This time is called penalty time for false alarm.

However, in UWB systems, such a sequential search can be very time consuming, as the number of cells is very large. This problem can be overcome by a new algorithm that we call "sequential block search". The key idea here is to divide the possible search space, which contains the cells, into several blocks, where each of the blocks contains a number of signal cells. We then first perform a quick test to check if the whole block contains a signal cell, or not. Once we have identified the block that contains the signal, a more detailed (sequential) search is performed in that block; for details, see [25]. Simulations show that acquisition can be achieved (with 90% probability) in less than $10\mu s$. This can be shortened even further if the search space is restricted, e.g., by exploiting knowledge from a beacon signal.

VI. Performance results

In this section, we analyze the performance of our system in multipath and interference. The performance of the system was simulated in “typical” UWB channels, which were developed within the IEEE 802.15.3a UWB standardization activities and are described in detail in [27]. We distinguish between four different types of channels (called CM1, CM2, CM3, and CM4). CM1 describes line-of-sight (LOS) scenarios with distances between TX and RX of less than 4m; CM2 and CM3 describe non-LOS scenarios at distances 0-4, and 4-10m, respectively. CM4 is valid for heavy multipath environments.

Figure 10 shows the probability for obtaining a successful link. A “successful” link means that acquisition is obtained successfully, and the packet error probability (over the ensemble of different channels) is less than 8%. For CM1, the mean coverage distance is about 10 m. The 10% outage distance (meaning that 8% packet error rate or less is guaranteed in 90% of all channels) is $7m$. For heavy multipath (CM4) these values decrease to 7 and 4m, respectively.

Figure 11 shows the analogous curves for a data rate of 200Mbit/s. Due to the higher rate, two parallel data streams are used. The time hopping codes for the two data streams are identical, but offset in delay by one chip. In

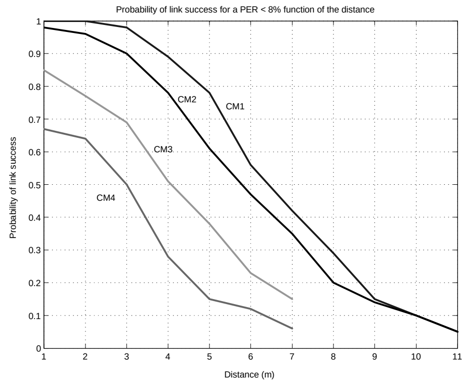

Fig. 11. Probability of link success as a function of distance for the 200Mbit/s mode.

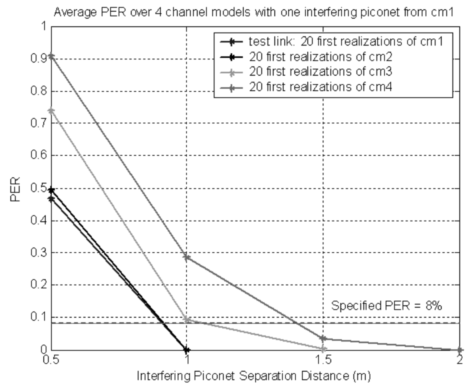

Fig. 12. Packet error rate as a function of the distance of interfering piconet in CM 1.

an AWGN channel, those codes would remain orthogonal, and the performance should be worsened only by 3dB (since the E_b/N_0 is decreased). However, in a multipath channel, the temporally offset codes lose their orthogonality, which worsens the performance. One way to remedy this situation is to use different (not just offset) hopping codes. However, this decreases the number of possible simultaneous piconets. Another approach would be the use of the scheme of [29], which retains the orthogonality of codes even in delay-dispersive channels.

Figures 12 and 13 show the performance when two users (independent piconets) are operating simultaneously. The desired users are located at half the distance that gives the 90% outage probability (i.e., there is a 6dB margin with respect to the single-user case); shadowing is not considered in that graph. We find that an “interfering piconet” can be at a distance from the victim receiver of about 1m (if the desired piconet is operating in CM1 or CM2), or 1.5m (if the desired piconet is operating in CM3 or CM4). The performance does not depend on which channel model is used for the interfering piconet.

Table 1 shows the coexistence of our system with other communications devices, obeying various narrowband standards. We find that if the UWB transmitter emits with the full power allowed by the FCC, it can significantly interfere with other communications devices. A suppression of about 15dB is necessary to allow coexistence within

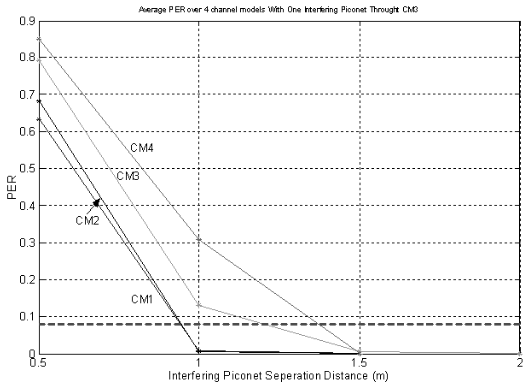

Fig. 13. Packet error rate as a function of the distance of interfering piconet in CM 3.

a 1m range. We achieve this suppression with the spectral shaping as described in Sec. 3.3.

System	*Desired*	*Achieved*	*FCC Mask*
$802.11a$	*-88dBm*	*-90dBm*	*-75dBm*
$802.11b$	*-82dBm*	*-85dBm*	*-70dBm*
$802.15.1$	*-76dBm*	*-95dBm*	*-80dBm*
$802.15.3$	*-81dBm*	*-85dBm*	*-70dBm*
$802.15.4$	*-91dBm*	*-95dBm*	*-80dBm*

Table 1: Coexistence for other systems

Finally, we also analyzed the resistance of the UWB system to interference *from* other communications devices. We found that again, a minimum distance of 1m is sufficient to allow operation with less than 8% PER.

VII. Summary and Conclusions

We have presented a UWB communications system based on time-hopping impulse radio. This system uses only baseband components, while still being compatible with FCC requirements, and providing a flexible shaping of the transmit spectrum in order to accommodate future requirements by other spectrum governing agencies, as well as not interfere with 802.11a wireless LANs and other communications receivers in the microwave range. Our system can sustain data rates of 110Mbit/s at 15m in AWGN channels, and 4-7m in multipath channels. It is also resistant to interference from other UWB users, as well as interference from wireless LANs, microwave ovens, and other interferers.

References

[1] J. D. Taylor, ed., *Introduction to Ultra -Wideband Radar Systems*. Boca Ranton, FL: CRC Press, first ed., 1995.

[2] R. A. Scholtz, “Multiple access with time-hopping impulse modulation,” in *MILCOM*, oct 1993.

[3] M. Z. Win and R. A. Scholtz, “Impulse radio: How it works,” *IEEE Comm. Lett.*, vol. 2, pp. 36–38, Feb 1998.

[4] M. Z. Win and R. A. Scholtz, "Ultra -wide bandwidth time-hopping spread-spectrum impulse radio for wireless multiple -access communications," *IEEE Trans. Comm.*, vol. 48, pp. 679–691, Apr 2000.

[5] S. S. Kolenchery, J. K. Townsend, and J. A. Freebersyser, "A novel impulse radio network for tactical military wireless communications," in *Milcom*, vol. 1, pp. 59–65, oct 1998. Boston, MA.

[6] M. Ho, L. Taylor, and G. Aiello, "UWB technology for wireless video networking," in *Int. Conference on Consumer Electronics, ICCE*, pp. 18 –19, 2001.

[7] C. J. Le Martret and G. B. Giannakis, "All-digital impulse radio for MUI/ISI-resilient transmissions through frequency-selective multipath channels," in *Milcom*, vol. 2, pp. 655–659, Oct 2000. Los Angeles, CA.

[8] J. Conroy, J. L. LoCicero, and D. R. Ucci, "Communication techniques using monopulse waveforms," in *Milcom*, vol. 2, pp. 1181–1185, Oct 1999. Atlantic City, NJ.

[9] A. R. Forouzan, M. Nasiri-Kenari, and J. A. Salehi, "Performance analysis of ultrawideband time-hopping code division multiple access systems: uncoded and coded schemes," in *Proc. Int. Conf. Comm.*, vol. 10, pp. 3017–3021, Jun 2001. Helsinki, FINLAND.

[10] D. Cassioli, M. Z. Win, F. Vatalaro, and A. F. Molisch, "Effects of spreading bw on the performance of uwb rake receivers," in *Proc. Int. Conf. Comm. 2003*, pp. 3545–3549, 2003.

[11] E. Fishler and H. V. Poor, "On the tradeoff between two types of processing gain," in *Proc. 40th Annual Allerton Conference on Communication, Control, and Computing*, 2002.

[12] Federal Communications Commission, "First report and order 02-48," 2002.

[13] *First Int. Symposium on Ultrawideband Systems and Technologies*. Baltimore, MA.

[14] *First International Workshop on Ultrawideband Systems*. Oulu, Finland.

[15] L. Zhao, A. M. Haimovich, and H. Grebel, "Performance of ultra-wideband communications in the presence of interference," in *Proc. Int. Conf. Comm.*, vol. 10, pp. 2948 –2952, Jun 2001. Helsinki, FINLAND.

[16] F. Ramirez-Mireles, "Performance of ultrawideband ssma using time hopping and m-ary ppm," *IEEE J. Selected Areas Comm.*, vol. 19, pp. 1186 –1196, Jun 2001.

[17] M. Z. Win and R. A. Scholtz, "On the energy capture of ultra -wide bandwidth signals in dense multipath environments," *IEEE Comm. Lett.*, vol. 2, pp. 245–247, Sept 1998.

[18] D. Cassioli, M. Z. Win, and A. F. Molisch, "The ultra-wide bandwidth indoor channel - from statistical model to simulations," *IEEE Journal on Selected Areas Communications*, vol. 20, pp. 1247–1257, 2002.

[19] A. Batra et al., "Multi-band OFDM physical layer proposal," 2003. Document IEEE 802.15-03/267r2.

[20] J. McCorkle et al., "Xtreme spectrum cpf document," 2003. Document IEEE 802.15-03/154r0.

[21] V. G. Subramanian and B. Hajek, "Broadband fading channels: signal burstiness and capacity," *IEEE Trans. Information Theory*, vol. 48, pp. 809–827, 2002.

[22] A. F. Molisch, M. Miyake, and J. Zhang, "Time hopping versus frequency hopping in ultrawideband systems," in *Proc. IEEE PACRIM 2003*, p. in press, 2003.

[23] Y. Wu, A. F. Molisch, S. Y. Kung, and J. Zhang, "Impulse radio pulse shaping for ultra-wide bandwidth uwb systems," in *Proc. PIRMC 2003*, p. in press, 2003.

[24] Y. P. Nakache and A. F. Molisch, "Spectral shape of uwb signals Űinfluence of modulation format, multiple access scheme and pulse shape," in *Proc. VTC 2003 spring*, pp. 2510–2514, 2003.

[25] S. Gesizi, E. Fishler, H. Kobayashi, H. V. Poor, and A. F. Molisch, "A rapid acquisition technique for impulse radio," in *Proc. IEEE PACRIM 2003*, p. in press, 2003.

[26] H. Sheng, P. Orlik, A. M. Haimovich, L. Cimini, and J. Zhang, "On the spectral and power requirements for ultra-wideband transmission," 2003.

[27] A. F. Molisch, J. R. Foerster, and M. Pendergrass, "Channel models for ultrawideband personal area networks," *IEEE Personal Communications Magazine*, p. in press, 2003.

[28] D. C. Cox, "Delay-doppler characteristics of multipath propagation at 910 MHz in a suburban mobile radio environment," *IEEE Trans. Antennas Propagation*, vol. AP-20, pp. 625–635, 1972.

[29] L. Yang and G. B. Giannakis, "Impulse radio multiple access through ISI channels with multi-stage block-spreading," in *Proc. UWB System Techn. 2002*, 2002.